

Small, coastal temperate rainforest watersheds dominate organic carbon transport to the northeast Pacific Ocean

G. McNicol^{1*}, E. Hood¹, D. E. Butman², S.E. Tank³, I.J.W. Giesbrecht^{4,5}, W. Floyd⁶, D. D'Amore⁷, J.B. Fellman¹, A. Cebulski^{8,#}, A. Lally⁸, H. McSorley⁸, and S.G. Gonzalez Arriola⁴

¹Department of Natural Sciences & Alaska Coastal Rainforest Center, University of Alaska Southeast, Juneau, AK

²School of Environmental and Forest Sciences & Department of Civil and Env. Engineering, University of Washington, Seattle

³Department of Biological Sciences, University of Alberta, Edmonton

⁴Hakai Institute, Vancouver, B.C., Canada

⁵School of Resource and Environmental Management, Simon Fraser University, Burnaby, BC, Canada

⁶Ministry of Forests, Nanaimo, BC, Canada

⁷U.S.D.A. Forest Service, Pacific Northwest Research Station, Juneau, AK

⁸Department of Geography, Vancouver Island University, Nanaimo, British Columbia, Canada

*now at: Department of Earth and Environmental Sciences, University of Illinois Chicago, IL

#now at: Department of Geography and Planning, University of Saskatchewan, Saskatoon, Saskatchewan, Canada

Corresponding author: E. Hood (ewhood@alaska.edu)

Key Points:

- The Northeast Pacific Coastal Temperate Rainforest drainage basin exports 3.5 Tg-C yr⁻¹ of dissolved organic carbon (DOC) to the ocean
- More than 50% of the land-to-ocean DOC flux is derived from small (median = 44 km²), coastal watersheds
- Watershed DOC yields peak in coastal B.C. where soil C, temperature, and precipitation combine to maximize terrestrial-aquatic DOC fluxes

44

45 **Abstract (150 words)**

46 The northeast Pacific Coastal Temperate Rainforest (NPCTR) extending from southeast Alaska
47 to northern California is characterized by high precipitation and among the largest stores of
48 recently fixed biological carbon on Earth. We show that 3.4 Tg-C yr^{-1} as DOC is exported from
49 the NPCTR drainage basin to the coastal ocean. More than 56% of this riverine DOC flux
50 originates from thousands of small ($10\text{-}10,000 \text{ km}^2$), coastal watersheds that comprise 22% of
51 the NPCTR drainage basin. The average DOC yield from NPCTR coastal watersheds (6.20 g-C
52 $\text{m}^{-2} \text{ yr}^{-1}$) exceeds that from Earth's tropical regions by roughly a factor of three. The highest
53 yields occur in small, coastal watersheds in the central NPCTR due to the balance of moderate
54 temperature, high precipitation, and high soil organic carbon stocks. These findings indicate that
55 DOC export from NPCTR watersheds may play an important role in heterotrophy within near-
56 shore marine ecosystems in the northeast Pacific.

57

58 **Plain Language Summary**

59 Carbon and water are dominant features within coastal temperate rainforests, which ring the
60 Pacific coast of northeast America and Asia, the southern coast of Chile, and western New
61 Zealand. The environmental conditions that support the largest stores of above ground biomass
62 on Earth also facilitate the movement of carbon through soils and streams to coastal zones. Here
63 we present the results of a large data synthesis to estimate the flux of organic carbon from the
64 land to sea along the Northeast Pacific Coastal Temperate Rainforest region that extends from
65 northern California through Southeast Alaska. We highlight that, although large rivers like the
66 Fraser River in Canada and the Columbia River in the United States drain a large proportion of
67 the region, the majority of the carbon entering coastal ecosystems originates from small, coastal
68 watersheds, highlighting the direct connection between terrestrial and estuarine ecosystems
69 within this region.

1 Introduction

The northeast Pacific Coastal Temperate Rainforest (NPCTR) is a region of dramatic elevation gradients including steep and subdued terrain and the largest remaining icefields in North America (Bidlack et al., 2021; O’Neel et al., 2015). Ecosystems within the NPCTR are characterized by slow and incomplete decomposition of organic carbon (OC), resulting in one of the densest terrestrial carbon stocks on Earth (McNicol et al., 2019). The regional proximity to frontal storms from the Gulf of Alaska leads to extreme rates of precipitation ($>6 \text{ m yr}^{-1}$ at high elevations) and an annual land-to-ocean freshwater flux of roughly 1300 km^3 (runoff = 0.9 m yr^{-1} ; Hill et al., 2015; Morrison et al., 2012). This freshwater discharge from the 1.4 M km^2 NPCTR drainage basin is 60% greater than that from the 3.4 M km^2 Mississippi River (Dai & Trenberth, 2002), and it provides an important vector for lateral transport of dissolved organic carbon (DOC) across the terrestrial-marine interface.

Quantifying the linked flows of water and DOC across coastal margins is crucial for understanding the flow of energy between terrestrial and estuarine ecosystems (Bauer et al., 2013; Hopkinson et al., 1998; Tank et al., 2012). Globally, small ($<10,000 \text{ km}^2$) mountainous watersheds are disproportionately important sources of terrestrial materials to the ocean (Milliman & Syvitski, 1992). In the NPCTR, the combination of large soil organic carbon (OC) stocks and high runoff rates facilitates rapid transfer of DOC to the coastal zone and mixing within the dominant currents that drive water flow in the Northeast Pacific Ocean. This organic matter provides metabolic support for coastal environments along the Riverine Coastal Domain, a narrow strip of buoyancy-driven boundary currents along western North America (Carmack et al., 2015).

Many small coastal watersheds in the northern and central NPCTR have extremely high yields of dissolved organic carbon ($10\text{--}40 \text{ g-C m}^2 \text{ yr}^{-1}$; D’Amore et al., 2015; Oliver et al., 2017). However, there are few regional scale, data-driven estimates for riverine DOC fluxes from temperate rainforest ecosystems to coastal environments. The southeast Alaska drainage basin, which includes the northern portion of the NPCTR, has been estimated to export $\sim 1 \text{ Tg-C yr}^{-1}$ as DOC (Edwards et al., 2021; Stackpoole, et al., 2017). In contrast, the Amazon River exports about 27 Tg-C yr^{-1} as DOC from an area ~ 50 times greater than the southeast Alaska drainage basin (Moreira-Turcq et al., 2003), illustrating that DOC yields from coastal temperate rainforest

(CTR) ecosystems may be larger than those from some tropical rainforests. However, runoff and DOC concentrations vary dramatically among the diverse watersheds of the NPCTR drainage basin (Giesbrecht et al., 2022), hindering efforts to scale DOC fluxes across this region.

Here we present the first comprehensive estimate for the flux of DOC entering the northeast Pacific across the perhumid and seasonal domains of the NPCTR coastal margin. We compile a continuous transboundary riverine DOC dataset to model long-term mean annual fluxes of DOC by watershed, explore the relative contributions of small coastal watersheds and larger continental river systems to the land-to-ocean flux of DOC within this C-rich ecoregion, and consider implications of this flow of DOC to downstream marine ecosystems.

2 Data and Methods

Watershed Characterization and DOC Data Compilation

Our study region extends from the Eel River watershed in northern California to the coastal watersheds of Glacier Bay National Park in southeast Alaska (Figure 1A). This region encompasses the perhumid NPCTR north of Vancouver Island, which receives substantial precipitation in every month of the year, as well as the seasonal NPCTR from Vancouver Island south, which is characterized by an annual summer-fall dry season. We used the watershed boundary dataset produced by Gonzalez Arriola et al. (2018), which merges existing government data products including U.S. Watershed Boundary Dataset 12-digit hydrologic units (U.S. Geological Survey, 2012) and British Columbia Freshwater Atlas Watershed Groups (Gonzalez Arriola et al., 2018) into seamless outlines with a consistent resolution across international (AK–BC–WA) and state (WA–OR–CA) boundaries. We omitted (~63,000) very small polygons (< 10km²), which were mostly tiny islets, together representing only 0.27% of the region. For each watershed, we used geographic information systems (GIS) to derive 17 attributes of climate and topography expected to control the watershed DOC yield (Table S1) based on previous work in this region (Giesbrecht et al., 2022).

Streamwater DOC concentration data were compiled from federal, provincial, and state databases, unpublished data, and previously published estimates, resulting in an initial dataset of 10,632 DOC measurements across 560 sites. This dataset was filtered to ensure that measurement location(s) closest to (but not within) the estuary were used when multiple sites

were present in a watershed, and that minimum criteria for watershed sample size ($n \geq 3$) and seasonal distribution were met (see Supplemental Text). Filtering resulted in a final dataset of 3,706 DOC measurements across 116 watersheds, with 2,758 observations from 108 small coastal watersheds and 948 observations from 8 continental watersheds (Table S2).

Estimates of Carbon Load and Yield

Continental watersheds: The 10 continental watersheds in the study domain (Fig. 1A) are gauged for discharge by federal agencies with DOC data available at the gauge site for 8 of 10 of the watersheds. In gauged watersheds, we used LOADEST (Runkel et al., 2004) to fit regression models for estimating annual loads ($Tg\ yr^{-1}$) at the most downstream gauge in each continental watershed ($n=3$; Table S3). Gauged loads were extrapolated to the watershed outlet using proportional discharge (see below for description and Table S3 for calculations). Loads previously calculated for U.S.-terminating watersheds ($n=5$; Edwards et al., 2021; Stets & Striegl, 2012) were used for extrapolation from gauge to outlet. For watersheds without DOC data (the Eel and Nass), loads were interpolated using the area-weighted load from nearby watersheds (Table S3). Annual yields ($g\ m^{-2}\ y^{-1}$) were then calculated by dividing outlet fluxes by the total watershed area.

Coastal watersheds: Because most small, coastal watersheds in the NPCTR are not gauged, loads and yields were calculated for all coastal watersheds with screened DOC concentration data ($n=108$, see above) using mean monthly runoff (1981-2010) estimates generated from a modification of the distributed climate water balance model (DCWBM) (Moore et al., 2012; see Supplemental Text). Mean monthly runoff was generated for each NPCTR watershed as a composite of modelled and gauged discharge. Mean monthly DOC yields were calculated as the product of mean monthly DOC concentration data and modeled monthly runoff. In cases where DOC data were not available for all months, monthly yields were scaled to annual yields by multiplying by the ratio of annual discharge to the sum of discharge during months for which DOC yields were computed. In addition, for the subset of coastal watersheds that met minimum LOADEST requirements (i.e., availability of gauged discharge data and a minimum number of DOC values; 23 of the 108 watersheds) and the 8 continental watersheds with DOC data, loads and yields were modeled via LOADEST as described above. A comparison of the two approaches confirmed similar results (Figure S1).

To extrapolate DOC yields to NPCTR coastal watersheds, we developed a model training dataset comprised of LOADEST yields and calculated watershed yields, using LOADEST yields where both were available. We used forward feature selection (FFS; Meyer et al. 2019) to identify the predictor subset that minimized the model mean absolute error (MAE) during leave-one-out cross validation after step-wise training of a random forest algorithm on all 17 watershed attribute predictors. An initial pair of, then single, predictors were added when they resulted in the lowest MAE, resulting in a final predictor set (Table S1) that was used to train a random forest model using all DOC yields that were calculated for coastal watersheds (Figure S2). Final model predictions were corrected for regression-to-the-mean effects common to decision tree algorithms using a linear spline function between observed and predicted DOC (Zhang & Lu, 2012), and yields were calculated for all NPCTR coastal watersheds using the final corrected model. Overall error in the modeled flux was computed by scaling the model mean absolute error estimated during cross validation to the model domain (Warner et al., 2019). Further methodological details are in the Supplemental text.

3 Results and Discussion

3.1 DOC export from the NPCTR drainage basin

We estimate that the total riverine DOC flux from the NPCTR drainage basin is 3.5 ± 0.92 Tg-C yr⁻¹ (Table 1). This constitutes about 1.6% of the annual DOC flux from global rivers to the ocean and roughly 10% of the total DOC flux to the Pacific Ocean (Dai et al., 2012; Li et al., 2017). In the context of North America, the flux of DOC from the NPCTR drainage basin exceeds the DOC fluxes from the three largest watersheds on the continent: the Mississippi (1.7-1.9 Tg-C yr⁻¹; Cai et al., 2015, Stackpoole et al., 2017), Mackenzie (1.38 Tg-C yr⁻¹, Holmes et al., 2012), and Yukon (1.47 Tg-C yr⁻¹; Holmes et al., 2012) river basins. Moreover, land-to-ocean DOC loss from the NPCTR drainage basin equates to more than half of annual DOC export from the conterminous United States (6.3 Tg-C yr⁻¹; Stets & Striegl, 2012) and more than 8% of the DOC flux from the entire North American continent (42.5 Tg-C yr⁻¹; Li et al., 2019). Within North America, the NPCTR drainage basin serves as a hotspot of DOC production, the export of which is closely connected to the coastal ocean. Our findings further suggest that the role of coastal temperate rainforest ecosystems in continental scale land-to-ocean DOC fluxes

warrants further examination in other CTR regions such as southern South America, New Zealand, and Japan.

Within the NPCTR drainage basin, the annual DOC flux is derived largely from coastal catchments, with 1.97 ± 0.85 Tg (56%) of the DOC flux coming from roughly 2700 small (median = 44 km^2) coastal watersheds that account for 22% of the NPCTR drainage basin area (Figure 2, Table 1). In contrast, only 1.57 ± 0.07 Tg (44%) of the DOC flux originates from the large continental watersheds that cross the Coast Mountains and account for the majority (78%) of the land area draining to the NPCTR coastal margin. The CTR zone within the NPCTR drainage basin, which includes abundant runoff from glaciers and icefields, thus serves as the primary driver of the land-to-ocean DOC flux in this region. Within the small watersheds of the CTR zone, the perhumid ecoregion, which is characterized higher annual precipitation distributed evenly across the year, had a higher annual DOC flux (1.26 Tg) compared to the seasonal ecoregion (0.71 Tg), which experiences an extended dry season during summer.

The spatial distribution of the riverine DOC flux from the NPCTR drainage basin is important because the Alaska Coastal Current originates close to the Columbia River mouth and transports freshwater and solutes northward to the productive near-shore marine ecosystems of the Gulf of Alaska (Figure 1; Stabeno et al., 1995). On a regional basis, British Columbia in the geographic center of the NPCTR had the largest annual DOC flux (1.74 Tg C; Table 1), followed by the contiguous U.S. (1.04 Tg C; 62% from the Columbia River Basin), and the watersheds draining into coastal southeast Alaska (0.76 Tg C). Our annual DOC flux estimate for southeast Alaska and transboundary watersheds of the BC/Alaska panhandle is notably smaller than a recent estimate of 1.12 Tg yr^{-1} by Edwards et al. (2021), who modeled DOC concentration and streamflow at the watershed scale. Our more conservative estimate of NPCTR DOC flux may arise from our model underestimating the exceptionally high DOC yields from small, outer coast watersheds in the center of our study domain (e.g. Oliver et al., 2017; Figure S3) due to a paucity of training data within this region (Figure S2).

3.2 Carbon yields

The range of magnitudes for our modeled watershed DOC yields ($1\text{-}29 \text{ g-C m}^{-2} \text{ yr}^{-1}$; Table 1) agrees with measured DOC yields from our study region including the central coast of British

Columbia (Oliver et al., 2017) and southeast Alaska (D'Amore et al., 2015), as well as similar coastal temperate rainforest watersheds in Chile (Pérez-Rodríguez & Biester, 2022). Moreover, our yield estimate for southeast Alaska is consistent with recent modeled yields of DOC ($6.2 \text{ g-C m}^{-2} \text{ yr}^{-1}$; Edwards et al., 2021) and total organic carbon (dissolved + particulate OC; $12.7 \text{ g-C m}^{-2} \text{ yr}^{-1}$; Stackpoole et al., 2017) for this region. The substantially higher modeled TOC yield of Stackpoole et al. (2017) results from the fact that particulate organic carbon (POC) can constitute more than 50% of the total riverine OC flux in the glacier-dominated watersheds found in the region (Bhatia et al., 2013; Hood et al., 2020).

The average DOC yield from the entire NPCTR drainage basin ($2.4 \text{ g-C m}^{-2} \text{ yr}^{-1}$; Table 1) is higher than the average DOC yield from Earth's tropical latitudes ($30^{\circ}\text{N} - 30^{\circ}\text{S}$) of $2.13 \text{ g-C m}^{-2} \text{ yr}^{-1}$ (Huang et al., 2012). The importance of small watersheds to this regional DOC flux is exemplified by the DOC yield from the NPCTR coastal watersheds ($6.20 \text{ g-C m}^{-2} \text{ yr}^{-1}$), and particularly the perhumid CTR ($7.30 \text{ g-C m}^{-2} \text{ yr}^{-1}$), exceeding that for the large continental river basins ($1.23 \text{ g-C m}^{-2} \text{ yr}^{-1}$) by a factor of 5-6x. The DOC yield from the NPCTR coastal watersheds exceeds that for the boreal forest dominated landscapes of Finland ($4.5 \text{ g-C m}^{-2} \text{ yr}^{-1}$; Räike et al., 2015) and Norway ($3.0 \text{ g-C m}^{-2} \text{ yr}^{-1}$; de Wit et al., 2015) as well as the peatland-rich landscape of Great Britain ($5.0 \text{ g-C m}^{-2} \text{ yr}^{-1}$; Williamson et al., 2021). Moreover, the highest DOC yields from outer-coast watersheds of the NPCTR ($20\text{-}30 \text{ g-C m}^{-2} \text{ yr}^{-1}$; Figure 2) are within the lower end of the range of DOC yields from peat-dominated, high-standing tropical islands in southeast Asia ($26\text{-}96 \text{ g-C m}^{-2} \text{ yr}^{-1}$; Baum et al., 2007; Moore et al., 2013; Wit et al., 2015), which have among the highest watershed DOC yields yet reported.

Within North America, the DOC yields we report for the NPCTR coastal watersheds are generally higher than those documented for watersheds in other ecoregions including agricultural ($0.3\text{-}2.3 \text{ g-C m}^{-2} \text{ yr}^{-1}$; Royer & David, 2005), blackwater swamp ($3.3\text{-}6.2 \text{ g-C m}^{-2} \text{ yr}^{-1}$; Avery et al., 2003; Leech et al., 2016), temperate forest ($2\text{-}10 \text{ g-C m}^{-2} \text{ yr}^{-1}$; Campbell et al., 2000; Huntington & Aiken, 2013). Overall, our findings indicate that CTR ecosystems are a regional and global hotspot of DOC export to the ocean (Edwards et al., 2021; Oliver et al., 2017; Stackpoole, Butman, et al., 2017). Further, our findings underscore the importance of small coastal watersheds as drivers of riverine material fluxes to the ocean (Destouni et al., 2008; Milliman & Syvitski, 1992; Warrick et al., 2015).

3.3 Drivers of organic carbon export from NPCTR ecosystems

Since Holocene glacial retreat, NPCTR landscapes have accumulated large stocks of organic carbon in both above ground biomass ($>150 \text{ Mg C ha}^{-1}$; DellaSala et al., 2022) and soils (mean 228 Mg C ha^{-1} equal to 2% of the soil OC stock in North America; McNicol et al., 2019). These OC stocks serve as source pools for riverine DOC via leaching of both live biomass (Behnke et al., 2022) and soil organic matter (D'Amore et al., 2015; Fellman et al., 2008). In particular, low relief areas of the NPCTR harbor abundant peatlands and forested wetlands that have a tight hydrological connection to stream networks and thus play an outsized role in the transfer of DOC between terrestrial and aquatic ecosystems similar to other temperate ecosystems (Creed et al., 2003; Inamdar & Mitchell, 2006; Laudon et al., 2004).

The NPCTR coastal margin is also characterized by high rates of specific discharge, particularly in the perhumid northern portion of the NPCTR where mean annual runoff ranges from $\sim 1\text{--}7 \text{ m yr}^{-1}$ (Giesbrecht et al., 2022). This elevated freshwater flux amplifies the positive relationship between soil C stocks and riverine DOC export (Aitkenhead & McDowell, 2000; Tank et al., 2018) within the NPCTR. Runoff from the NPCTR is driven largely by high levels of precipitation in the Coast Ranges extending from the Pacific Northwest to Alaska (Luce et al., 2013; Shanley et al., 2015). However, volume loss from the more than $20,000 \text{ km}^2$ of glacier ice in the northern portion of the NPCTR also contributes substantially to streamflow (Neal et al., 2010). Glacier runoff in this region is projected to increase in coming decades (Bliss et al., 2014), and thus heavily glacierized watersheds will continue to contribute substantially to land-to-ocean DOC fluxes despite having small terrestrial C stocks and correspondingly low riverine DOC concentrations (Hood et al., 2009). Additionally, newly exposed post-glacial soils in the northern NPCTR can accumulate OC at rates exceeding $1 \text{ Mg C ha}^{-1} \text{ yr}^{-1}$ (Chandler, 1943), the leaching of which contributes DOC to streams.

Within the NPCTR, the highest DOC yields occur along the outer coast between northern Vancouver Island in Canada and the southern Alexander Archipelago in southeast Alaska (Figure 1B). The latitudinal temperature gradient across our study region appears to play an important role in the storage and release of soil C to streams. The most dense stores of soil OC ($>500 \text{ Mg C ha}^{-1}$) occur in the Alexander Archipelago of southeast Alaska, where cool year-round temperatures and prolonged soil saturation inhibit decomposition of soil organic matter

(McNicol et al., 2019). However, the largest watershed DOC yields occur further south consistent with the idea that temperature is an important control on DOC production within the soil profile (Christ & David, 1996; D’Amore et al., 2010; Ziegler et al., 2017). In addition, the transition from the perhumid rainforest to the seasonal rainforest north of Vancouver Island occurs coincident with the peak in watershed DOC yields suggesting that episodic drying and rewetting of soils also facilitates DOC production and increases lateral DOC export at the watershed scale (Tiwari et al., 2022; Tunaley et al., 2016). South of Vancouver Island, watershed DOC yields are limited by relatively lower soil C stocks (Sun et al., 2004) and catchment water yields compared to the northern and central NPCTR. In this context, the central NPCTR is a “sweet spot” for land-to-ocean DOC transport as a result of positive interactions between key environmental variables such as temperature, precipitation, and soil OC that control DOC export.

The highest DOC yields we modeled occurred in the smallest watersheds in our study domain (largely < 50 km²). This is consistent with the idea the large OC stocks in upland and particularly wetland soils within small watersheds in the NPCTR have a larger proportional influence (compared to larger watersheds) on streamwater DOC concentrations due to their consistent hydrological connectivity to the stream network (Covino, 2017) and short water residence times, particularly during storm events, which minimize instream processing and uptake of DOC (Raymond et al., 2016). Thus, small catchments along the outer coast of the NPCTR play an outsized role in regional terrestrial OC export partly because their streamwater carbon biogeochemistry directly reflects inputs of OC from above and below ground biomass stores (Marx et al., 2017). The magnitude of watershed DOC fluxes from NPCTR modeled here and documented previously (D’Amore et al., 2015; Edwards et al., 2021; Oliver et al., 2017) highlights the importance of accounting for small, wetland-rich, near-coastal watersheds in regional riverine DOC flux calculations (Williamson et al., 2021).

Projected future increases in precipitation and temperature across the central and northern NPCTR (Lader et al., 2020; Shanley et al., 2015) can be expected to increase rates of soil carbon export as DOC from coastal watersheds. Within individual watersheds, streamwater DOC concentrations across the region increase sharply with discharge (D’Amore et al., 2010; Fellman et al., 2020; Hood et al., 2020) indicating that watershed DOC export is broadly transport (water) limited and will increase with precipitation. The frequency of landfalling atmospheric river

precipitation events is projected to increase substantially (50-600%) in the NPCTR in coming decades (Gao et al., 2015), and extreme high flow events strongly enhance DOC export at the watershed scale (Yoon & Raymond, 2012). Thus, a higher incidence of atmospheric rivers within the NPCTR will increase the relative importance of storm events, which dominate the annual DOC export budget of forested watersheds (Fellman et al., 2009; Raymond & Saiers, 2010), in the regional DOC export budget.

3.4 Fate of riverine DOC in NPCTR marine ecosystems

Riverine export of DOC can be an important C source for near-shore marine ecosystems, where terrigenous DOC can be either mineralized to CO₂ or incorporated into coastal microbial food webs (Fichot & Benner, 2014; Medeiros et al., 2017). In the NPCTR, both microbial uptake and flocculation contribute to riverine DOC losses in estuarine ecosystems (Fellman et al., 2010; St. Pierre et al., 2020). The importance of terrestrial DOC as a source of C and energy for near-shore ecosystems is magnified by the fact that a majority of the small, DOC-rich coastal watersheds in the perhumid NPCTR drain into sheltered inside waters and fjords. As a result, the residence time and potential for biological processing of DOC in estuarine ecosystems adjacent to the NPCTR is substantially higher compared to coastlines where runoff from rivers enters the open ocean and is rapidly transported offshore (Edwards et al., 2021).

Across near-shore sites fed by forested and glacial streams in the NPCTR, marine microbial communities can metabolize a substantial (22-44%) fraction of inflowing riverine DOC, suggesting that the non-conservative behavior of DOC in river plumes is partially a result of biological removal (Fellman et al., 2010). This C subsidy for marine food webs is particularly important during the autumn and winter months, when runoff is highest and primary production in near-shore marine ecosystems is limited by shorter days and deep, turbulent mixing (St. Pierre et al., 2020). Assimilation of riverine terrestrial organic matter into marine food webs has been demonstrated in near-shore environments (e.g. Connolly et al., 2009). In the NPCTR, riverine DOC can serve as the primary source of organic matter in near-shore ecosystems (St. Pierre et al., 2022). Moreover, terrestrial C has been shown to account for a substantial proportion (12-50%) of the biomass C of copepods, birds, and fish in CTR fjord ecosystems in Chile and Alaska (Arimitsu et al., 2018; Vargas et al., 2011), however it is unclear what proportion of this C enters marine food webs as DOC compared to POC.

Climate change may alter the flow of OC across the land-ocean interface in the NPCTR. Glacier lake outburst floods (Harrison et al., 2018) and landslides associated with both atmospheric rivers (Darrow et al., 2022) and glacier recession are projected to increase in frequency (Holm et al., 2004). These events deliver large volumes of sediment via rivers to the coast, where freshwater plumes can extend more than 50 km down fjord ecosystems and impact coastal C cycling and marine food webs (Geertsema et al., 2022; Meerhoff et al., 2019). Perturbations to riverine sediment transport driven by extreme events will also affect the form of riverine OC. Currently, DOC is the dominant vector of land-to-ocean OC transport in the NPCTR, accounting for more than 80% of OC export in forested watersheds and up to 50% of OC export in heavily glacierized watersheds (Hood et al., 2020). However, during extreme high flow events, fluxes of POC increase far more rapidly than those for DOC due to the mobilization of sediment from terrestrial and aquatic ecosystems (Dhillon & Inamdar, 2014). Thus, an increase in the incidence of glacier lake outburst floods, extreme precipitation events, and landslides within the NPCTR will amplify the role of POC as a vector for the transfer of OC to near-shore marine ecosystems.

4 Conclusions

We present the first unified estimate for the flux of riverine DOC to the NW Pacific and show that the NPCTR drainage basin is a global hotspot of land-to-ocean organic carbon transport, representing ~10% of the total DOC exported to the Pacific Ocean. Our model results suggest that majority of this DOC flux originates from small, coastal watersheds, with the highest watershed yields occurring on the outer coast in central British Columbia. Watershed fluxes of POC and inorganic C remain unquantified, however, they may contribute an additional 50% to the regional riverine carbon flux (Stackpoole et al., 2017). The large land-to-ocean OC fluxes we quantify may play important roles in the NPCTR C cycle by stimulating heterotrophic production in near-shore marine ecosystems during seasons of limited primary production and by determining whether the NPCTR functions as a C sink or source at regional scales.

Acknowledgments

Croix Fylpaa provided assistance with data retrieval and organization. Joanna Li Yung Lung provided assistance with watershed flux modeling. Molly Tankersley designed Figure 1. Jason Berge, Mark Scott, and Malysa Maurer collected DOC samples at Water Survey of

Canada gauging stations thanks to arrangements made with David Hutchinson. Isabelle Desmarais, Rob White, Maartje Korver, and Emily Haughton collected DOC samples for Hakai Institute. Dave Rolston and Robin Pike assisted with sample collection. Megan Behnke commented on an early manuscript draft. Funding was provided by the U.S. National Science Foundation grants through the Coastal Margins Research Coordination Network (DEB-1557186) and Alaska EPSCoR (OIA-1757348). The Tula Foundation supported sampling in BC and networking activities, and the University of Washington College of Environment provided workshop facilities that supported paper development.

Open Research

Site locations, DOC data, discharge data, and modeled DOC fluxes are available for review in the supplemental material (files ds01-ds03) and will be made available via a DOI link to a FAIR-aligned data repository upon paper acceptance.

379

380 **Table 1.** Watershed information and DOC fluxes and yields by watershed type (small coastal
 381 versus large continental; rows 1-4) and sub-region (rows 4-7). Small coastal watersheds are
 382 further subdivided into the perhumid and seasonal CTR ecoregions. The S.E. Alaska and
 383 Contiguous U.S. sub-regions include significant areas of British Columbia due to transboundary
 384 watersheds.

Sub-Region	Watershed Count	Watershed Area (km ²)	Annual DOC Flux (Tg-C yr ⁻¹)	DOC Yield (range; g-C m ⁻² yr ⁻¹)
Small Coastal	2695	317,768	1.97 ± 0.85	6.2 (1.3-28.9)
<i>Perhumid</i>	1913	171,509	1.26	7.3 (2.1-28.8)
<i>Seasonal</i>	782	146,258	0.71	4.9 (1.3-28.9)
Large Continental	10	1,125,294	1.57 ± 0.07	1.4 (0.9-3.0)
S.E. Alaska	1172	154,365	0.76	4.9 (1.1-26.5)
British Columbia	1243	455,592	1.74	3.8 (1.4-28.9)
Contiguous U.S.	290	833,105	1.04	1.2 (1.0-28.0)
NPCTR drainage basin total	2705	1,443,062	3.5 ± 0.92	2.4 (1.0-28.9)

385

386

387

388

389

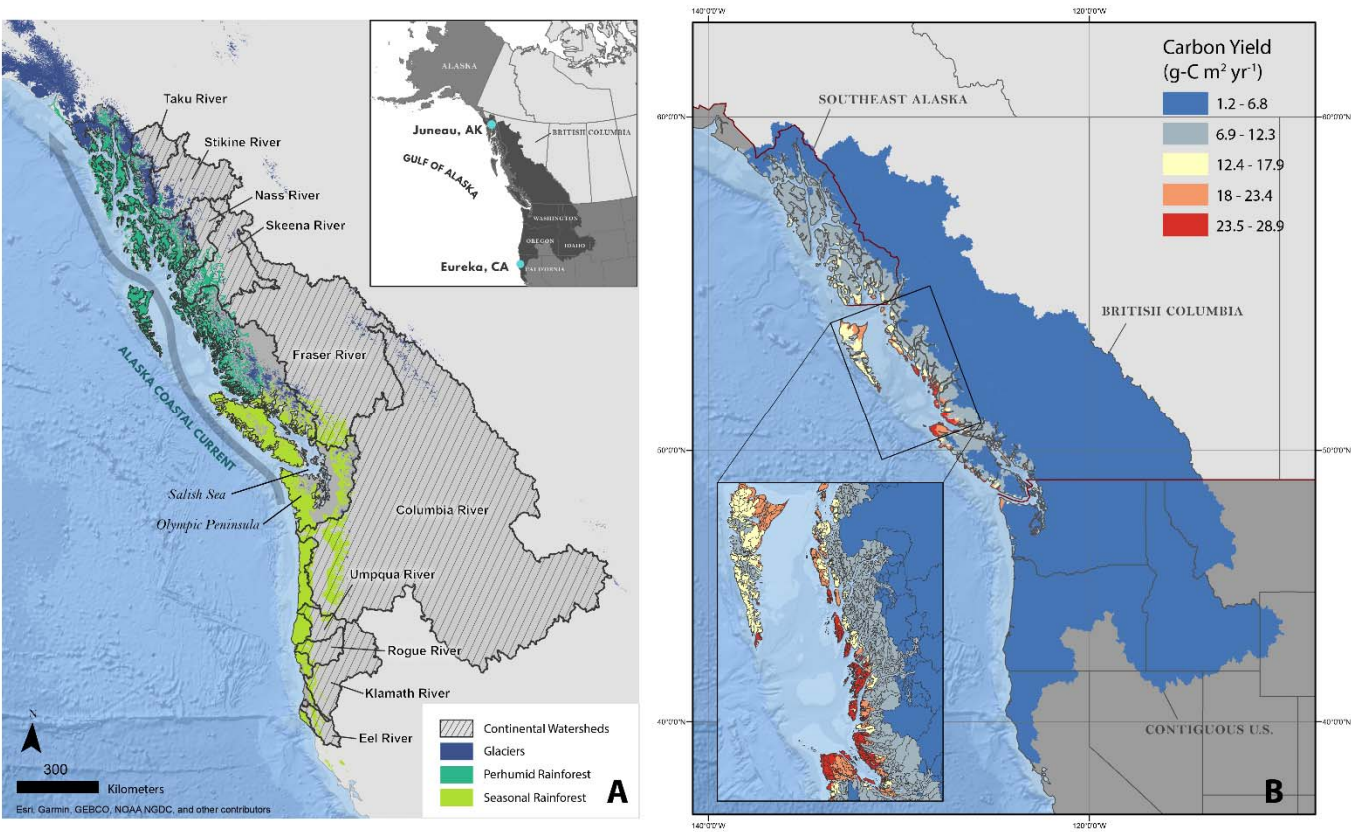
390

Figure Captions

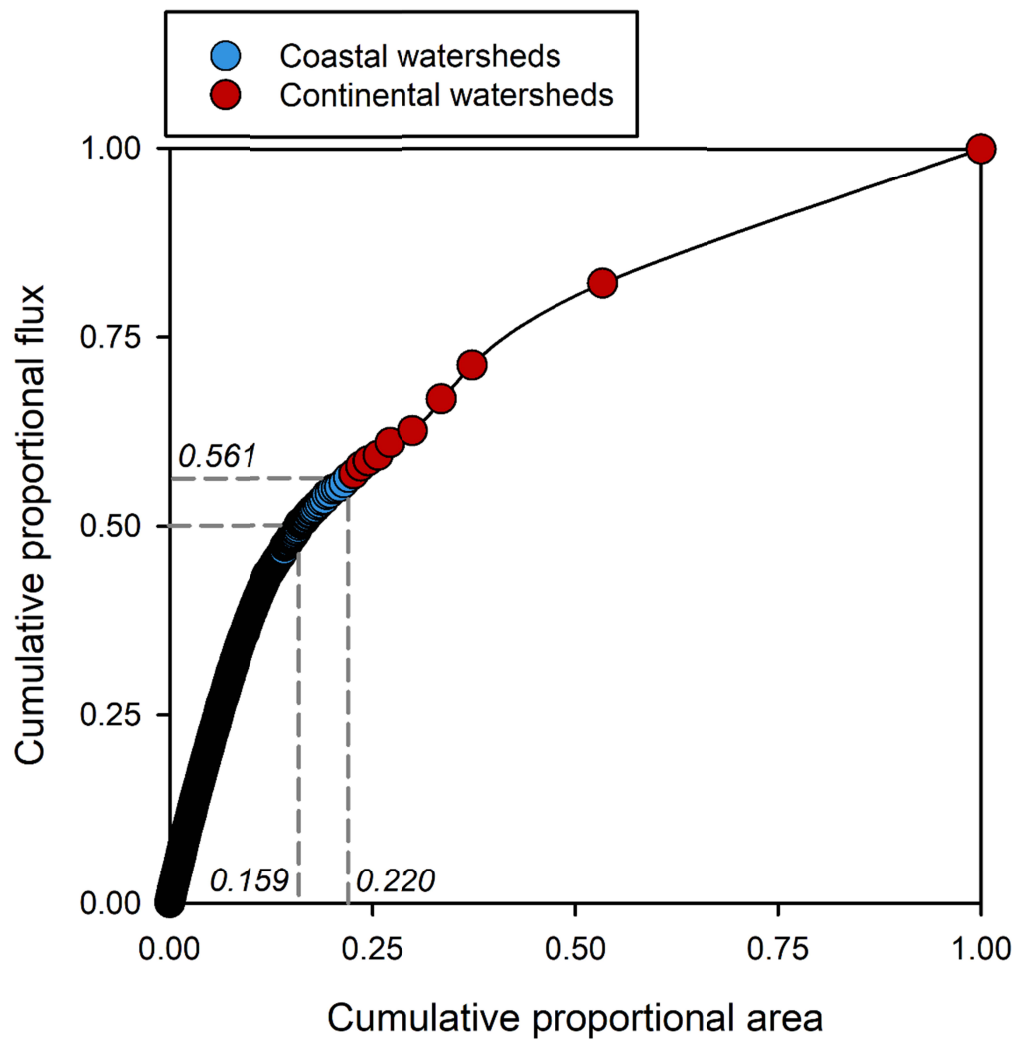
Figure 1. Location and extent of the Northeast Pacific Coastal Temperate Rainforest (colored zones) in the context of the larger NPCTR drainage basin, which includes small coastal watersheds (thin black lines) and ten large continental watersheds (heavy black lines) used in this analysis (A). Range of modeled watershed carbon yields across the study region, which includes the S.E. Alaska, British Columbia, and Contiguous U.S. sub-regions (B).

Figure 2. Cumulative proportion of the regional DOC flux versus cumulative proportional watershed area. Blue dots represent small coastal watersheds ($n = 2695$), and red dots represent the 10 continental watersheds.

402 Figure 1.



407 **Figure 2.**



408

409

410

411

References

- Aitkenhead, J. A., & McDowell, W. H. (2000). Soil C:N ratio as a predictor of annual riverine DOC flux at local and global scales. *Global Biogeochemical Cycles*, 14(1), 127–138.
<https://doi.org/10.1029/1999GB900083>
- Albers, S. J. (2018). tidyhydat: Extract and Tidy Canadian Hydrometric Data. *Journal of Open Source Software*, 3(21), 511.
- Arimitsu, M. L., Hobson, K. A., Webber, D. N., Piatt, J. F., Hood, E. W., & Fellman, J. B. (2018). Tracing biogeochemical subsidies from glacier runoff into Alaska's coastal marine food webs. *Global Change Biology*, 24(1), 387–398. <https://doi.org/10.1111/gcb.13875>
- Arino, O., Ramos Perez, J. J., Kalogirou, V., Bontemps, S., Defourny, P., & Van Bogaert, E. (2012). *Global Land Cover Map for 2009 (GlobCover 2009)*. Retrieved from:
<https://doi.org/10.1594/PANGAEA.787668>
- Avery, G. B., Willey, J. D., Kieber, R. J., Shank, G. C., & Whitehead, R. F. (2003). Flux and bioavailability of Cape Fear River and rainwater dissolved organic carbon to Long Bay, southeastern United States. *Global Biogeochemical Cycles*, 17(2), 1042. <https://doi.org/10.1029/2002GB001964>
- Bauer, J. E., Cai, W.-J., Raymond, P. A., Bianchi, T. S., Hopkinson, C. S., & Regnier, P. A. G. (2013). The changing carbon cycle of the coastal ocean. *Nature*, 504(7478), 61–70.
<https://doi.org/10.1038/nature12857>
- Baum, A., Rixen, T., & Samiaji, J. (2007). Relevance of peat draining rivers in central Sumatra for the riverine input of dissolved organic carbon into the ocean. *Estuarine, Coastal and Shelf Science*, 73(3–4), 563–570. <https://doi.org/10.1016/j.ecss.2007.02.012>
- Behnke, M. I., Fellman, J. B., D'Amore, D. V., Gomez, S. M., & Spencer, R. G. M. (2022). From canopy to consumer: what makes and modifies terrestrial DOM in a temperate forest. *Biogeochemistry*.
<https://doi.org/10.1007/s10533-022-00906-y>
- Bhatia, M. P., Das, S. B., Xu, L., Charette, M. A., Wadham, J. L., & Kujawinski, E. B. (2013). Organic carbon export from the Greenland ice sheet. *Geochimica et Cosmochimica Acta*, 109, 329–344.
<https://doi.org/10.1016/j.gca.2013.02.006>
- Bidlack, A. L., Bisbing, S. M., Buma, B. J., Diefenderfer, H. L., Fellman, J. B., Floyd, W. C., et al. (2021). Climate-Mediated Changes to Linked Terrestrial and Marine Ecosystems across the Northeast Pacific Coastal Temperate Rainforest Margin. *BioScience*, 71(6), 581–595.
<https://doi.org/10.1093/biosci/biaa171>

444 Bliss, A., Hock, R., & Radić, V. (2014). Global response of glacier runoff to twenty-first century climate
 445 change. *Journal of Geophysical Research: Earth Surface*, 119(4), 717–730.
 446 <https://doi.org/10.1002/2013JF002931>

447 Breiman, L. (2001). Random Forests. *Machine Learning*, 45(1), 5-32.
 448 <https://doi.org/10.1023/A:1010933404324>

449 Burnham, K. P., & Anderson, D. R. (2002). *Model selection and multi-model inference: A practical*
 450 *information-theoretic approach*. New York: Springer.

451 Cai, Y., Guo, L., Wang, X., & Aiken, G. (2015). Abundance, stable isotopic composition, and export fluxes
 452 of DOC, POC, and DIC from the Lower Mississippi River during 2006-2008. *Journal of Geophysical*
 453 *Research: Biogeosciences*, 120(11), 2273–2288. <https://doi.org/10.1002/2015JG003139>

454 Campbell, J. L., Hornbeck, J. W., McDowell, W. H., Buso, D. C., Shanley, J. B., & Likens, G. E. (2000).
 455 Dissolved organic nitrogen budgets for upland, forested ecosystems in New England.
 456 *Biogeochemistry*, 49(2), 123–142.

457 Carmack, E., Winsor, P., & Williams, W. (2015). The contiguous panarctic Riverine Coastal Domain: A
 458 unifying concept. *Progress in Oceanography*, 139, 13–23.
 459 <https://doi.org/10.1016/j.pocean.2015.07.014>

460 Chandler, R. F. (1943). The Time Required for Podzol Profile Formation as Evidenced by the Mendenhall
 461 Glacial Deposits Near Juneau, Alaska. *Soil Science Society of America Journal*, 7(C), 454–459.
 462 <https://doi.org/10.2136/sssaj1943.036159950007000C0077x>

463 Christ, M. J., & David, M. B. (1996). Temperature and moisture effects on the production of dissolved
 464 organic carbon in a Spodosol. *Soil Biology and Biochemistry*, 28(9), 1191–1199.
 465 [https://doi.org/10.1016/0038-0717\(96\)00120-4](https://doi.org/10.1016/0038-0717(96)00120-4)

466 Connolly, R. M., Schlacher, T. A., & Gaston†, T. F. (2009). Stable isotope evidence for trophic subsidy of
 467 coastal benthic fisheries by river discharge plumes off small estuaries. *Marine Biology Research*,
 468 5(2), 164–171. <https://doi.org/10.1080/17451000802266625>

469 Covino, T. (2017). Hydrologic connectivity as a framework for understanding biogeochemical flux
 470 through watersheds and along fluvial networks. *Geomorphology*, 277, 133–144.
 471 <https://doi.org/10.1016/j.geomorph.2016.09.030>

472 Creed, I. F., Sanford, S. E., Beall, F. D., Molot, L. A., & Dillon, P. J. (2003). Cryptic wetlands: integrating
 473 hidden wetlands in regression models of the export of dissolved organic carbon from forested
 474 landscapes. *Hydrological Processes*, 17(18), 3629–3648. <https://doi.org/10.1002/hyp.1357>

475 Dai, A., & Trenberth, K. E. (2002). Estimates of Freshwater Discharge from Continents: Latitudinal and
 476 Seasonal Variations. *Journal of Hydrometeorology*, 3(6), 660–687. [https://doi.org/10.1175/1525-](https://doi.org/10.1175/1525-7541(2002)003<0660:EOFDFC>2.0.CO;2)
 477 7541(2002)003<0660:EOFDFC>2.0.CO;2

478 Dai, M., Yin, Z., Meng, F., Liu, Q., & Cai, W.-J. (2012). Spatial distribution of riverine DOC inputs to the
 479 ocean: an updated global synthesis. *Current Opinion in Environmental Sustainability*, 4(2), 170–
 480 178. <https://doi.org/10.1016/j.cosust.2012.03.003>

481 D’Amore, D. V., Fellman, J. B., Edwards, R. T., & Hood, E. (2010). Controls on dissolved organic matter
 482 concentrations in soils and streams from a forested wetland and sloping bog in southeast
 483 Alaska. *Ecohydrology*, 3(3), 249–261. <https://doi.org/10.1002/eco.101>

484 D’Amore, D. V., Edwards, R. T., Herendeen, P. A., Hood, E., & Fellman, J. B. (2015). Dissolved Organic
 485 Carbon Fluxes from Hydropedologic Units in Alaskan Coastal Temperate Rainforest Watersheds.
 486 *Soil Science Society of America Journal*, 79(2), 378–388.
 487 <https://doi.org/10.2136/sssaj2014.09.0380>

488 Darrow, M. M., Nelson, V. A., Grilliot, M., Wartman, J., Jacobs, A., Baichtal, J. F., & Buxton, C. (2022).
 489 Geomorphology and initiation mechanisms of the 2020 Haines, Alaska landslide. *Landslides*,
 490 19(9), 2177–2188. <https://doi.org/10.1007/s10346-022-01899-3>

491 De Cicco, L. A., Hirsch, R. M., Lorenz, D., & Watkins, W. D. (2022). dataRetrieval: R packages for
 492 discovering and retrieving water data available from Federal hydrologic web services, v.2.7.11.

493 DellaSala, D. A., Gorelik, S. R., & Walker, W. S. (2022). The Tongass National Forest, Southeast Alaska,
 494 USA: A Natural Climate Solution of Global Significance. *Land*, 11(5), 717.
 495 <https://doi.org/10.3390/land11050717>

496 Destouni, G., Hannerz, F., Prieto, C., Jarsjö, J., & Shibuo, Y. (2008). Small unmonitored near-coastal
 497 catchment areas yielding large mass loading to the sea. *Global Biogeochemical Cycles*, 22(4),
 498 GB4003. <https://doi.org/10.1029/2008GB003287>

499 Dhillon, G. S., & Inamdar, S. (2014). Storm event patterns of particulate organic carbon (POC) for large
 500 storms and differences with dissolved organic carbon (DOC). *Biogeochemistry*, 118(1–3), 61–81.
 501 <https://doi.org/10.1007/s10533-013-9905-6>

502 Edwards, R. T., D’Amore, D. V., Biles, F. E., Fellman, J. B., Hood, E. W., Trubilowicz, J. W., & Floyd, W. C.
 503 (2021). Riverine Dissolved Organic Carbon and Freshwater Export in the Eastern Gulf of Alaska.
 504 *Journal of Geophysical Research: Biogeosciences*, 126(1).
 505 <https://doi.org/10.1029/2020JG005725>

- Fellman, J. B., D'Amore, D. V., Hood, E., & Boone, R. D. (2008). Fluorescence characteristics and biodegradability of dissolved organic matter in forest and wetland soils from coastal temperate watersheds in southeast Alaska. *Biogeochemistry*, 88(2), 169–184.
<https://doi.org/10.1007/s10533-008-9203-x>
- Fellman, J. B., Hood, E., Edwards, R. T., & D'Amore, D. V. (2009). Changes in the concentration, biodegradability, and fluorescent properties of dissolved organic matter during stormflows in coastal temperate watersheds. *Journal of Geophysical Research*, 114(G1).
<https://doi.org/10.1029/2008JG000790>
- Fellman, J. B., Spencer, R. G. M., Hernes, P. J., Edwards, R. T., D'Amore, D. V., & Hood, E. (2010). The impact of glacier runoff on the biodegradability and biochemical composition of terrigenous dissolved organic matter in near-shore marine ecosystems. *Marine Chemistry*, 121(1–4), 112–122. <https://doi.org/10.1016/j.marchem.2010.03.009>
- Fellman, J. B., Hood, E., Behnke, M. I., Welker, J. M., & Spencer, R. G. M. (2020). Stormflows drive stream carbon concentration, speciation, and dissolved organic matter composition in coastal temperate rainforest watersheds. *Journal of Geophysical Research: Biogeosciences*, 125(9).
<https://doi.org/10.1029/2020JG005804>
- Fichot, C. G., & Benner, R. (2014). The fate of terrigenous dissolved organic carbon in a river-influenced ocean margin. *Global Biogeochemical Cycles*, 28(3), 300–318.
<https://doi.org/10.1002/2013GB004670>
- Gao, Y., Lu, J., Leung, L. R., Yang, Q., Hagos, S., & Qian, Y. (2015). Dynamical and thermodynamical modulations on future changes of landfalling atmospheric rivers over western North America. *Geophysical Research Letters*, 42(17), 7179–7186. <https://doi.org/10.1002/2015GL065435>
- Geertsema, M., Menounos, B., Bullard, G., Carrivick, J. L., Clague, J. J., Dai, C., et al. (2022). The 28 November 2020 Landslide, Tsunami, and Outburst Flood – A Hazard Cascade Associated With Rapid Deglaciation at Elliot Creek, British Columbia, Canada. *Geophysical Research Letters*, 49(6).
<https://doi.org/10.1029/2021GL096716>
- Giesbrecht, I. J. W., Tank, S. E., Frazer, G. W., Hood, E., Gonzalez Arriola, S. G., Butman, D. E., et al. (2022). Watershed Classification Predicts Streamflow Regime and Organic Carbon Dynamics in the Northeast Pacific Coastal Temperate Rainforest. *Global Biogeochemical Cycles*, 36(2), e2021GB007047. <https://doi.org/10.1029/2021GB007047>

- Gonzalez Arriola, S. G., Giesbrecht, I. J. W., Biles, F. E., & D'Amore, D. V. (2018). Watersheds of the northern Pacific coastal temperate rainforest margin [Data set]. Hakai Institute. <https://doi.org/10.21966/1.715755>
- Gregorutti, B., Michel, B., & Saint-Pierre, P. (2017). Correlation and variable importance in random forests. *Statistics and Computing*, 27(3), 659–678. <https://doi.org/10.1007/s11222-016-9646-1>
- Harrison, S., Kargel, J. S., Huggel, C., Reynolds, J., Shugar, D. H., Betts, R. A., et al. (2018). Climate change and the global pattern of moraine-dammed glacial lake outburst floods. *The Cryosphere*, 12(4), 1195–1209. <https://doi.org/10.5194/tc-12-1195-2018>
- Hill, D. F., Bruhis, N., Calos, S. E., Arendt, A., & Beamer, J. (2015). Spatial and temporal variability of freshwater discharge into the Gulf of Alaska. *Journal of Geophysical Research: Oceans*, 120(2), 634–646. <https://doi.org/10.1002/2014JC010395>
- Holm, K., Bovis, M., & Jakob, M. (2004). The landslide response of alpine basins to post-Little Ice Age glacial thinning and retreat in southwestern British Columbia. *Geomorphology*, 57(3–4), 201–216. [https://doi.org/10.1016/S0169-555X\(03\)00103-X](https://doi.org/10.1016/S0169-555X(03)00103-X)
- Holmes, R. M., McClelland, J. W., Peterson, B. J., Tank, S. E., Bulygina, E., Eglinton, T. I., et al. (2012). Seasonal and annual fluxes of nutrients and organic matter from large rivers to the Arctic Ocean and surrounding seas. *Estuaries and Coasts*, 35(2), 369–382. <https://doi.org/10.1007/s12237-011-9386-6>
- Hood, E., Fellman, J., Spencer, R. G. M., Hernes, P. J., Edwards, R., D'Amore, D., & Scott, D. (2009). Glaciers as a source of ancient and labile organic matter to the marine environment. *Nature*, 462(7276), 1044–1047. <https://doi.org/10.1038/nature08580>
- Hood, E., Fellman, J. B., & Spencer, R. G. M. (2020). Glacier loss impacts riverine organic carbon transport to the ocean. *Geophysical Research Letters*, 47(19). <https://doi.org/10.1029/2020GL089804>
- Hopkinson, C. S., Buffam, I., Hobbie, J., Vallino, J., Perdue, M., Eversmeyer, B., et al. (1998). Terrestrial inputs of organic matter to coastal ecosystems: An intercomparison of chemical characteristics and bioavailability. *Biogeochemistry*, 43(3), 211–234. <https://doi.org/10.1023/A:1006016030299>
- Huang, T.-H., Fu, Y.-H., Pan, P.-Y., & Chen, C.-T. A. (2012). Fluvial carbon fluxes in tropical rivers. *Current Opinion in Environmental Sustainability*, 4(2), 162–169. <https://doi.org/10.1016/j.cosust.2012.02.004>

- Huntington, T. G., & Aiken, G. R. (2013). Export of dissolved organic carbon from the Penobscot River basin in north-central Maine. *Journal of Hydrology*, 476, 244–256.
<https://doi.org/10.1016/j.jhydrol.2012.10.039>
- Inamdar, S. P., & Mitchell, M. J. (2006). Hydrologic and topographic controls on storm-event exports of dissolved organic carbon (DOC) and nitrate across catchment scales. *Water Resources Research*, 42(3). <https://doi.org/10.1029/2005WR004212>
- Jarvis, A., Reuter, H. I., Nelson, A., & Guevara, E. (2008) Hole-filled SRTM for the globe Version 4, available from the CGIAR-CSI SRTM 90m Database (<http://srtm.csi.cgiar.org>).
- Lader, R., Bidlack, A., Walsh, J. E., Bhatt, U. S., & Bieniek, P. A. (2020). Dynamical Downscaling for Southeast Alaska: Historical Climate and Future Projections. *Journal of Applied Meteorology and Climatology*, 59(10), 1607–1623. <https://doi.org/10.1175/JAMC-D-20-0076.1>
- Laudon, H., Kohler, S., & Buffam, I. (2004). Seasonal TOC export from seven boreal catchments in northern Sweden. *Aquatic Sciences - Research Across Boundaries*, 66(2), 223–230.
<https://doi.org/10.1007/s00027-004-0700-2>
- Leech, D. M., Ensign, S. H., & Piehler, M. F. (2016). Spatiotemporal patterns in the export of dissolved organic carbon and chromophoric dissolved organic matter from a coastal, blackwater river. *Aquatic Sciences*, 78(4), 823–836. <https://doi.org/10.1007/s00027-016-0474-3>
- Li, M., Peng, C., Wang, M., Xue, W., Zhang, K., Wang, K., et al. (2017). The carbon flux of global rivers: A re-evaluation of amount and spatial patterns. *Ecological Indicators*, 80, 40–51.
<https://doi.org/10.1016/j.ecolind.2017.04.049>
- Li, M., Peng, C., Zhou, X., Yang, Y., Guo, Y., Shi, G., & Zhu, Q. (2019). Modeling Global Riverine DOC Flux Dynamics From 1951 to 2015. *Journal of Advances in Modeling Earth Systems*, 11(2), 514–530.
<https://doi.org/10.1029/2018MS001363>
- Luce, C. H., Abatzoglou, J. T., & Holden, Z. A. (2013). The Missing Mountain Water: Slower Westerlies Decrease Orographic Enhancement in the Pacific Northwest USA. *Science*, 342(6164), 1360–1364. <https://doi.org/10.1126/science.1242335>
- Marx, A., Dusek, J., Jankovec, J., Sanda, M., Vogel, T., van Geldern, R., et al. (2017). A review of CO₂ and associated carbon dynamics in headwater streams: A global perspective: Carbon Dioxide in Headwater Streams. *Reviews of Geophysics*, 55(2), 560–585.
<https://doi.org/10.1002/2016RG000547>
- McCabe, G. J., & Markstrom, S. L. (2007). *A monthly water-balance model driven by a graphical user interface*.

598 McNicol, G., Bulmer, C., D'Amore, D., Sanborn, P., Saunders, S., Giesbrecht, I., et al. (2019). Large,
 599 climate-sensitive soil carbon stocks mapped with pedology-informed machine learning in the
 600 North Pacific coastal temperate rainforest. *Environmental Research Letters*, 14(1), 014004.
 601 <https://doi.org/10.1088/1748-9326/aaed52>

602 Medeiros, P. M., Seidel, M., Gifford, S. M., Ballantyne, F., Dittmar, T., Whitman, W. B., & Moran, M. A.
 603 (2017). Microbially-Mediated Transformations of Estuarine Dissolved Organic Matter. *Frontiers*
 604 *in Marine Science*, 4. <https://doi.org/10.3389/fmars.2017.00069>

605 Meerhoff, E., Castro, L. R., Tapia, F. J., & Pérez-Santos, I. (2019). Hydrographic and biological impacts of a
 606 glacial lake outburst flood (GLOF) in a Patagonian fjord. *Estuaries and Coasts*, 42(1), 132–143.
 607 <https://doi.org/10.1007/s12237-018-0449-9>

608 Meyer, H., Reudenbach, C., Hengl, T., Katurji, M., & Nauss, T. (2018). Improving performance of spatio-
 609 temporal machine learning models using forward feature selection and target-oriented
 610 validation. *Environmental Modelling & Software*, 101, 1-9.
 611 <https://www.sciencedirect.com/science/article/pii/S1364815217310976>

612 Milliman, J. D., & Syvitski, J. P. M. (1992). Geomorphic/Tectonic Control of Sediment Discharge to the
 613 Ocean: The Importance of Small Mountainous Rivers. *The Journal of Geology*, 100(5), 525–544.
 614 <https://doi.org/10.1086/629606>

615 Moore, R. D. D., Trubilowicz, J. W., & Buttle, J. M. (2012). Prediction of Streamflow Regime and Annual
 616 Runoff for Ungauged Basins Using a Distributed Monthly Water Balance Model1: Prediction of
 617 Streamflow Regime and Annual Runoff for Ungauged Basins Using a Distributed Monthly Water
 618 Balance Model. *JAWRA Journal of the American Water Resources Association*, 48(1), 32–42.
 619 <https://doi.org/10.1111/j.1752-1688.2011.00595.x>

620 Moore, S., Evans, C. D., Page, S. E., Garnett, M. H., Jones, T. G., Freeman, C., et al. (2013). Deep
 621 instability of deforested tropical peatlands revealed by fluvial organic carbon fluxes. *Nature*,
 622 493(7434), 660–663. <https://doi.org/10.1038/nature11818>

623 Moreira-Turcq, P., Seyler, P., Guyot, J. L., & Etcheber, H. (2003). Exportation of organic carbon from the
 624 Amazon River and its main tributaries. *Hydrological Processes*, 17(7), 1329–1344.
 625 <https://doi.org/10.1002/hyp.1287>

626 Morrison, J., Foreman, M. G. G., & Masson, D. (2012). A method for estimating monthly freshwater
 627 discharge affecting British Columbia coastal Waters. *Atmosphere-Ocean*, 50(1), 1–8.
 628 <https://doi.org/10.1080/07055900.2011.637667>

629 Neal, E. G., Hood, E., & Smikrud, K. (2010). Contribution of glacier runoff to freshwater discharge into
630 the Gulf of Alaska. *Geophysical Research Letters*, 37(6), L06404.
631 <https://doi.org/10.1029/2010GL042385>

632 Oliver, A. A., Tank, S. E., Giesbrecht, I., Korver, M. C., Floyd, W. C., Sanborn, P., et al. (2017). A global
633 hotspot for dissolved organic carbon in hypermaritime watersheds of coastal British Columbia.
634 *Biogeosciences*, 14(15), 3743–3762. <https://doi.org/10.5194/bg-14-3743-2017>

635 O’Neel, S., Hood, E., Bidlack, A. L., Fleming, S. W., Arimitsu, M. L., Arendt, A., et al. (2015). Icefield-to-
636 Ocean Linkages across the Northern Pacific Coastal Temperate Rainforest Ecosystem.
637 *BioScience*, 65(5), 499–512. <https://doi.org/10.1093/biosci/biv027>

638 Pebesma, E. (2018). Simple Features for R: Standardized Support for Spatial Vector Data. *The R Journal*,
639 10(1), 439-446.

640 Pérez-Rodríguez, M., & Biester, H. (2022). Sensitivity of river catchments to discharge-controlled
641 dissolved carbon export: a study of eight catchments in southern Patagonia. *Biogeochemistry*,
642 160(2), 177–197. <https://doi.org/10.1007/s10533-022-00947-3>

643 R Core Team. (2022). R: A Language and Environment for Statistical Computing. In. Vienna, Austria: R
644 Foundation for Statistical Computing.

645 Räike, A., Kortelainen, P., Mattsson, T., & Thomas, D. N. (2015). Long-term trends (1975–2014) in the
646 concentrations and export of carbon from Finnish rivers to the Baltic Sea: organic and inorganic
647 components compared. *Aquatic Sciences*. <https://doi.org/10.1007/s00027-015-0451-2>

648 Raymond, P. A., & Saiers, J. E. (2010). Event controlled DOC export from forested watersheds.
649 *Biogeochemistry*, 100(1–3), 197–209. <https://doi.org/10.1007/s10533-010-9416-7>

650 Raymond, P. A., Saiers, J. E., & Sobczak, W. V. (2016). Hydrological and biogeochemical controls on
651 watershed dissolved organic matter transport: pulse-shunt concept. *Ecology*, 97(1), 5–16.
652 <https://doi.org/10.1890/14-1684.1>

653 Royer, T. V., & David, M. B. (2005). Export of dissolved organic carbon from agricultural streams in
654 Illinois, USA. *Aquatic Sciences*, 67(4), 465–471. <https://doi.org/10.1007/s00027-005-0781-6>

655 Runkel, R. L., Crawford, C. G., & Cohn, T. A. (2004). *Load Estimator (LOADEST): A Fortran program for*
656 *estimating constituent loads in streams and rivers* (No. 4-A5). Reston, VA: U.S. Geological Survey
657 Techniques and Methods.

658 Shanley, C. S., Pyare, S., Goldstein, M. I., Alaback, P. B., Albert, D. M., Beier, C. M., et al. (2015). Climate
659 change implications in the northern coastal temperate rainforest of North America. *Climatic*
660 *Change*, 130, 155–170. <https://doi.org/10.1007/s10584-015-1355-9>

661 St. Pierre, K. A., Oliver, A. A., Tank, S. E., Hunt, B. P. V., Giesbrecht, I., Kellogg, C. T. E., et al. (2020).
 662 Terrestrial exports of dissolved and particulate organic carbon affect nearshore ecosystems of
 663 the Pacific coastal temperate rainforest. *Limnology and Oceanography*, 65(11), 2657–2675.
 664 <https://doi.org/10.1002/lno.11538>
 665 St. Pierre, K. A., Hunt, B. P. V., Giesbrecht, I. J. W., Tank, S. E., Lertzman, K. P., Del Bel Belluz, J., et al.
 666 (2022). Seasonally and Spatially Variable Organic Matter Contributions From Watershed, Marine
 667 Macrophyte, and Pelagic Sources to the Northeast Pacific Coastal Ocean Margin. *Frontiers in*
 668 *Marine Science*, 9, 863209. <https://doi.org/10.3389/fmars.2022.863209>
 669 Stabenow, P. J., Reed, R. K., & Schumacher, J. D. (1995). The Alaska Coastal Current: Continuity of
 670 transport and forcing. *Journal of Geophysical Research*, 100(C2), 2477.
 671 <https://doi.org/10.1029/94JC02842>
 672 Stackpoole, S. M., Butman, D. E., Clow, D. W., Verdin, K. L., Gaglioti, B. V., Genet, H., & Striegl, R. G.
 673 (2017). Inland waters and their role in the carbon cycle of Alaska. *Ecological Applications*, 27(5),
 674 1403–1420. <https://doi.org/10.1002/eap.1552>
 675 Stackpoole, S. M., Stets, E. G., Clow, D. W., Burns, D. A., Aiken, G. R., Aulenbach, B. T., et al. (2017).
 676 Spatial and temporal patterns of dissolved organic matter quantity and quality in the Mississippi
 677 River Basin, 1997–2013. *Hydrological Processes*, 31(4), 902–915.
 678 <https://doi.org/10.1002/hyp.11072>
 679 Stets, E., & Striegl, R. (2012). Carbon export by rivers draining the conterminous United States. *Inland*
 680 *Waters*, 2(4), 177–184. <https://doi.org/10.5268/IW-2.4.510>
 681 Sun, O. J., Campbell, J., Law, B. E., & Wolf, V. (2004). Dynamics of carbon stocks in soils and detritus
 682 across chronosequences of different forest types in the Pacific Northwest, USA: SOIL AND
 683 DETRITUS C DYNAMICS. *Global Change Biology*, 10(9), 1470–1481.
 684 <https://doi.org/10.1111/j.1365-2486.2004.00829.x>
 685 Tank, S. E., Frey, K. E., Striegl, R. G., Raymond, P. A., Holmes, R. M., McClelland, J. W., & Peterson, B. J.
 686 (2012). Landscape-level controls on dissolved carbon flux from diverse catchments of the
 687 circumboreal. *Global Biogeochemical Cycles*, 26(4), GB0E02.
 688 <https://doi.org/10.1029/2012GB004299>
 689 Tank, S. E., Fellman, J. B., Hood, E., & Kritzberg, E. S. (2018). Beyond respiration: Controls on lateral
 690 carbon fluxes across the terrestrial-aquatic interface. *Limnology and Oceanography Letters*.
 691 <https://doi.org/10.1002/lol2.10065>

- Tiwari, T., Sponseller, R. A., & Laudon, H. (2022). The emerging role of drought as a regulator of dissolved organic carbon in boreal landscapes. *Nature Communications*, 13(1), 5125. <https://doi.org/10.1038/s41467-022-32839-3>
- Tunaley, C., Tetzlaff, D., Lessels, J., & Soulsby, C. (2016). Linking high-frequency DOC dynamics to the age of connected water sources. *Water Resources Research*, 52(7), 5232–5247. <https://doi.org/10.1002/2015WR018419>
- U.S. Geological Survey. (n.d.). *USGS Watershed Boundary Dataset (WBD) for 2-digit Hydrologic Unit - 03 Shapefile (published 2012)*.
- Vargas, C. A., Martinez, R. A., San Martin, V., Aguayo, M., Silva, N., & Torres, R. (2011). Allochthonous subsidies of organic matter across a lake–river–fjord landscape in the Chilean Patagonia: Implications for marine zooplankton in inner fjord areas. *Continental Shelf Research*, 31(3), 187–201. <https://doi.org/10.1016/j.csr.2010.06.016>
- Wang, T., Hamann, A., Spittlehouse, D., & Carroll, C. (2016). Locally Downscaled and Spatially Customizable Climate Data for Historical and Future Periods for North America. *PLOS ONE*, 11(6), e0156720. <https://doi.org/10.1371/journal.pone.0156720>
- Warner, D. L., Bond-Lamberty, B., Jian, J., Stell, E., & Vargas, R. (2019). Spatial Predictions and Associated Uncertainty of Annual Soil Respiration at the Global Scale. *Global Biogeochemical Cycles*, 33(12), 1733–1745. <https://doi.org/10.1029/2019GB006264>
- Warrick, J. A., Melack, J. M., & Goodridge, B. M. (2015). Sediment yields from small, steep coastal watersheds of California. *Journal of Hydrology: Regional Studies*, 4, 516–534. <https://doi.org/10.1016/j.ejrh.2015.08.004>
- Williamson, J. L., Tye, A., Lapworth, D. J., Monteith, D., Sanders, R., Mayor, D. J., et al. (2021). Landscape controls on riverine export of dissolved organic carbon from Great Britain. *Biogeochemistry*. <https://doi.org/10.1007/s10533-021-00762-2>
- Wit, F., Müller, D., Baum, A., Warneke, T., Pranowo, W. S., Müller, M., & Rixen, T. (2015). The impact of disturbed peatlands on river outgassing in Southeast Asia. *Nature Communications*, 6(1), 10155. <https://doi.org/10.1038/ncomms10155>
- de Wit, H. A., Austnes, K., Hølen, G., & Dalsgaard, L. (2015). A carbon balance of Norway: terrestrial and aquatic carbon fluxes. *Biogeochemistry*, 123(1–2), 147–173. <https://doi.org/10.1007/s10533-014-0060-5>

722 Wright, M. N., & Ziegler, A. (2017). ranger: A Fast Implementation of Random Forests for High
 723 Dimensional Data in C++ and R. *Journal of Statistical Software*, 77(1), 1 - 17.
 724 <https://www.jstatsoft.org/index.php/jss/article/view/v077i01>

725 Yoon, B., & Raymond, P. A. (2012). Dissolved organic matter export from a forested watershed during
 726 Hurricane Irene. *Geophysical Research Letters*, 39(18), n/a-n/a.
 727 <https://doi.org/10.1029/2012GL052785>

728 Zhang, G., & Lu, Y. (2012). Bias-corrected random forests in regression. *Journal of Applied Statistics*,
 729 39(1), 151–160. <https://doi.org/10.1080/02664763.2011.578621>

730 Ziegler, S. E., Benner, R., Billings, S. A., Edwards, K. A., Philben, M., Zhu, X., & Laganière, J. (2017).
 731 Climate Warming Can Accelerate Carbon Fluxes without Changing Soil Carbon Stocks. *Frontiers*
 732 *in Earth Science*, 5. <https://doi.org/10.3389/feart.2017.00002>

733